Single-Step Synthesis of Ultrafine PLZT from Polymer Gel Precursor: Synthesis, Consolidation, and Dielectric Properties

S. Roy,*[,†] S. Bysakh,[†] M. L. N. Goswami,[‡] D. Jana,[§] and J. Subrahmanyam[†]

Defence Metallurgical Research Laboratory, DRDO, Hyderabad 500058, A.P., India, Department of Physics, Midnapore College, West Bengal 721101, India, and Department of Physics, Vidyasagar University, West Bengal 721102, India

Received August 10, 2006. Revised Manuscript Received October 12, 2006

Ultrafine $Pb_{0.93}La_{.07}Zr_{0.60}Ti_{0.40}O_3$ powder was synthesized by autoignition of a metal−polymer gel precursor on a hot plate at very low temperatures without an additional calcination step. The X-ray diffraction result of the as-burnt powder obtained after ignition showed the presence of rhombohedral lead lanthanum zirconate titanate (PLZT) with minute amounts of unreacted PbO. The average particle size calculated from the transmission electron microscopy micrograph of the as-burnt powder was 1.75 nm. The as-burnt ultrafine PLZT powder was sintered directly to 94 and 96% of its theoretical density at 1100 and 1200 °C without any additional calcination. The PLZT sample with 94% theoretical density and grain sizes 0.4−1.0 μm showed a very high dielectric permittivity of ∼5000 and a completely diffused phase transition near the Curie point. This sample exhibited a remnant polarization (P_r) of ∼34.6 μc/cm^2. The permittivity of the 1200 °C sintered sample decreases drastically to ∼800. Both of the sintered samples showed very low dielectric loss.

I. Introduction

Lanthanum-doped lead zirconate titanate (PLZT) materials are of significant practical and academic importance on account of their excellent piezoelectric ferroelectric, electrooptic, and pyroelectric properties.[1−5] A wide range of sensors, actuators, electrooptic devices, and transducers based on PLZT ceramics have been developed during the last few decades. The properties of PLZT materials are directly related to their crystal chemistry, homogeneity, and microstructure. It is very difficult to achieve a sintered density close to theoretical density via conventional ceramic routes, using mixed oxides as the starting material. The nonuniformity of the mixture of raw materials results in localized grain growth and thus a wide distribution of grain sizes. This problem, together with some undesirable features of sintered lead-based perovskite oxides, such as nonstoichiometry in composition and poor microstructure, is due to the loss in lead content during calcinations and sintering processes as a result of high volatility of PbO at elevated temperatures. Therefore, it is desirable to process lead zirconate titanate (PZT)-based ceramic materials at as low a temperature as possible. An approach is the use of ultrafine ceramic powders as the starting material, which may be synthesized via several chemistry-based novel synthesis techniques such as citrate gel combustion route,[6] polyvinyl alcohol gel route,[7] hydrothermal reaction,[8] homogeneous precipitation,[9] and alkoxide hydrolysis.[10,11] Synthesis of single and binary metal oxides from metal−polyvinyl alcohol (M−PVA) gel precursor has been one of the most focused soft chemical methods in the past few years.[7,12−13] The usual way to obtain nanoceramic oxides is by the reaction of the mixed-metal salt solution in proper stoichiometric ratio with aqueous PVA solution in certain concentration and evaporation of the mixture to get M−PVA gel. The gel is then burnt on a hot plate to get a black carbonaceous powder followed by calcination at different temperatures ≥600 °C to obtain nanoparticles with different particle sizes. In some cases, the oven-dried gel is directly calcined to get nanosized ceramic powder.

We worked on a similar chemical route but modified the procedure to obtain a M−PVA gel with the proper PVA: NO_3^- ratio such that the gel undergoes an autoignition reaction on the hot plate kept at ∼180 °C and burns completely to obtain nanosized ceramic powders, leaving negligible carbonaceous residue. The PVA plays the dual role of a complexing agent to the metal ions, resulting in a

* Corresponding author. Tel: 040-24586663. Fax: 040-24340683. E-mail: r_subir@dmrl.ernet.in.
† Defense Metallurgical Research Laboratory.
‡ Indian Institute of Technology.
§ Vidyasagar University.

(1) Moulson, A. J.; Herbert, J. M. *Electroceramics: Materials, Properties, Applications*; Chapman & Hall: London, 1990.
(2) Jaffe, B.; Cook, W. R.; Jaffe, H. *Piezoelectric Ceramics*; Academic Press: New York, 1971.
(3) Haertling, G. H.; Land, C. E. *J. Am. Ceram. Soc.* **1971**, *54* (1), 1−11.
(4) Liu, T.; Heaps, J. D.; Tufte, O. N. *Ferroelectrics* **1972**, *3*, 281−85.
(5) Choi, J. J.; Ryu, J.; Kim, H. E. *J. Am. Ceram. Soc.* **2001**, *84* (7), 1465−69.
(6) Scheafer, J.; Sigmund, W.; Roy, S.; Aldinger, F. *J. Mater. Res.* **1997**, *12* (10), 2518−2521.
(7) Wang, J.; Liu, Q.; Xue, D.; Li, F. *J. Mater. Sci. Lett.* **2002**, *21*, 1059.
(8) Chen, H.; Ma, J.; Jhu, B.; Yuhong, C. *J. Am. Ceram. Soc.* **1993**, *76* (3), 625−29.
(9) Roy, S.; Bysakh, S.; Subrahmanyam, J. *J. Mater. Res.* **2006**, *21* (4), 856−863.
(10) Wu, A.; Vilarinh, P. M.; Miranda Salvado, I. M.; Baptista, J. L. *J. Am. Ceram. Soc.* **2000**, *83* (6), 1379−85.
(11) Zhai, J.; Chena, H. *J. Appl. Phys.* **2003**, *94* (1), 589−593.
(12) Saha, S.; Pramanik, P. *Nanostruct. Mater.* **1997**, *8*, 29−36.
(13) Yamamoto, S.; Kakihana, M.; Kato, S.; *J. Alloys Compd.* **2000**, *297*, 81−86.

10.1021/cm061884+ CCC: $37.00 © 2007 American Chemical Society
Published on Web 04/24/2007

homogeneous distribution of the metal ions in the solution and as a fuel.

The present method offers several advantages over the other chemical synthesis techniques commonly used for synthesizing nanoceramic oxides: (i) It avoids any additional calcination step that is often required in other synthesis techniques to burn out the carbonacious part completely from the powder obtained after combustion.[6,7,9−13] (ii) The ceramic oxide particles obtained by this method are much finer and assume a narrower size distribution than that obtained in most other techniques.[6−13] (iii) The precursor gel directly crystallizes as the perovskite PLZT phase without undergoing undesirable intermediate pyrochlore phase formation, the control of which is very critical to the processing of lead-based perovskite dielectric and ferroelectric materials.[10,11,14] (iv) The exothermicity, i.e., the heat of autoignition of M−PVA gel is many times lower than the other autoignition/combustion reactions involving glycine,[15] urea,[16] hydrazine,[17] etc. This low heat of reaction eventually helps to avoid particle coarsening and minimizes the agglomeration. Particle coarsening and particle agglomeration are common problems in combustion syntheses. (v) The residual carbon content in the as-burnt powder obtained after autoignition is negligible and hence the as-burnt powder could be directly used for sintering without any further calcination.

The reduction of particle size of ferroelectrics seems to have a significant effect on polarization. The effect of grain size in nanometer[18] and micrometer[19] level on the electrical properties of ferroelectrics is different, as the ferroelectric structures of a particular material in theses two scales are different. Hence, beside the synthesis, a study of the electrical properties of the synthesized product in the consolidated form would be of great fundamental interest. In the present work, we report for the first time the autoignition of M−PVA gel, leading to a single-step synthesis of ultrafine PLZT particles. The autoignitable M−PVA gel was obtained by simple adjustment of NO_3^-/PVA ratio without adding any combustible material such as urea, sucrose, citric acid, glycine, etc. In addition to synthesis, consolidation, and study of its dielectric, ferroelectric properties are also discussed in the present article.

II. Experimental Section

The PLZT precursor solutions were synthesized from the starting materials of $Pb(NO_3)_2$, $La(NO_3)_3$, $ZrCl_4$, and $TiCl_4$ in the stoichiometric 0.93:0.07:0.60:0.40 molar ratios. $ZrCl_4$ (dissolved in deionized water) and $TiCl_4$ (diluted in 6.0 M HCl) were mixed together and precipitated as hydrated oxides by hydrolysis with NH_4OH in cold water (2−5 °C). The precipitate was washed repeatedly in deionized water to remove the chloride ions and dissolved in 1.5 M HNO_3 in cold conditions to produce mixed oxynitrate solutions containing $ZrO(NO_3)_2$ and $TiO(NO_3)_2$. This solution was mixed with aqueous $Pb(NO_3)_2$ and $La(NO_3)_3$ solutions in requisite amounts to prepare 0.2 M stock solution with respect to PLZT. The addition of excess lead, usually used to prevent lead loss at high processing temperatures, was avoided, as the extra lead that remains after sintering gets deposited at the grain boundaries and deteriorates the electrical properties. For a batch of 30 g of PLZT powder, 500 mL of mixed nitrate/oxynitrate solution was placed in a 3000 mL Borosil beaker and 1000 mL of a 5 wt % aqueous solution of PVA of 14 000 average molecular weight was then added. Extra nitric acid was added to produce different sets of gel with a varied nitrate/polymer ratio (R_{np}). The value of R_{np} was kept between 0.28 and 0.56. The water in this solution was evaporated at 70 °C to produce the metal−PVA gel, which was burnt at 180 °C to produce nanostructured PLZT. The autoignition of the M−PVA gel depends largely on the value of R_{np}. The X-ray diffraction (XRD) of the powder samples was carried out in a Philips X-ray diffractometer using $Cu_{k\alpha}$ radiation. Thermal analysis for the dried gel was carried out using a TG−DTA analyzer (TA Instruments, SDT 2960) in air between 30 and 1000 °C with a heating rate of 10 °C /min in air. Differential scanning calorimetric measurements of the as-dried powders were carried out using a DSC analyzer (TA Instruments, DS2920) between 30 and 600 °C with varied heating rate in air. The powder samples for TEM observation were prepared by dispersing the powder in methanol and adding a few drops of the suspension on a carbon-coated TEM grid. A FEI Tecnai 20T TEM was used for observation. The powders were die-pressed under a pressure of 500 MPa and subsequently sintered in a lead-rich atmosphere at 1100 and 1200 °C for 4 h in air. The growth of the particle size of the polycrystalline samples in the pellet (diameter ∼8 mm and thickness ∼1.02 mm) was studied by scanning electron microscopy (SEM). For electrical measurements, the samples were coated with fine silver paint on either side of the pellets, and necessary ohmic contacts were made. Quantitative elemental analysis of the sintered sample was done by electron probe microanalysis (EPMA) on the diamond-polished and carbon-coated pellet.

Measurements of the dielectric constant (ϵ) and the dissipation factor (tan δ) of the sintered samples were carried out at various frequencies (1 kHz to 1 MHz) and at different temperatures (30−300 °C) using an Agilent Precision LCR meter (model 4210). The room-temperature polarization was obtained from the saturated $P-E$ hysteresis loop, obtained with the help of a laboratory modified Sawyer−Tower circuit at 50 Hz.

III. Results and Discussion

A. Thermal Analyses of the M−PVA Gel. Thermogravimetric analysis (TGA) and differential thermal analysis (DTA) measurements were carried out to study the thermal behavior of the gel, and the respective curves are shown in Figure 1. The figure shows the DTA and TGA curves of the as-dried gel between 25 and 985 °C in air. The TGA shows weight loss in several steps. The initial weight loss of the gel in air between 25 and 130 °C is attributed to the loss of moisture. The appearance of a small exothermic peak at 136 °C, associated with weight loss between 130 and 150 °C in the TGA curve, is possibly due to the decomposition of NO_3^- adsorbed to the surface of the M−PVA gel. The sharp exothermic peak at 478 °C is accompanied by a sharp weight loss that is observed in the TGA curve. This corresponds to the ignition of the gel. This thermal behavior of the gel can

(14) Zang, M.; Salvado, I. M. M.; Vilarinho, P. M. *J. Am. Ceram. Soc.* **2003**, *86* (5), 775−81.
(15) Chick, L. A.; Pederson, L. R.; Maupin, G. D.; Bates, J. L.; Thomas, L. E.; Exarhos, G. J. *Mater. Lett.* **1990**, *10* (1−2), 6−12.
(16) Kingsley, J. J.; Patil, K. C. *Mater. Lett.* **1988**, *6*, 427.
(17) Ravindranathan, P.; Patil, K. C. *Am. Ceram. Soc. Bull.* **1987**, *66* (4), 688−92.
(18) Zhao, Z.; Buscaglia, V.; Viviani, M.; Buscaglia, M. T.; Mitoseriu, L.; Testino, A.; Nygren, M.; Johnsson, M.; Nanni, P. *Phys. Rev. B* **2004**, *70*, 024107.
(19) Arlt, G.; Hennings D.; With, G. *J. Appl. Phys.* **1984**, *58* (4), 1619−25.

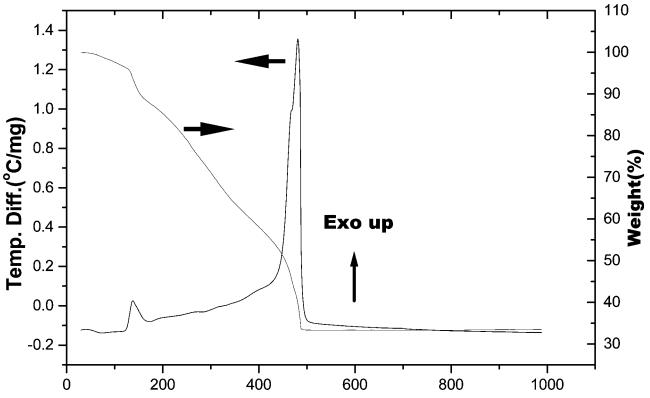

Figure 1. DTA and TGA curves for the oven-dried M−PVA gel of $R_{np} = 0.49$, showing a single-step conversion to the product phase.

be compared with the thermal behavior of the precursor gel synthesized for the citrate gel combustion, where the decomposition of the gel is realized by the appearance of a single sharp exothermic peak in DTA.[6] This indicates the complete conversion of the M−PVA gel to the product phase in a single step. Above 485 °C, there is no further weight loss in the TGA, which suggests that the gel burns completely by the ignition reaction. This also conforms to our finding of negligible amounts of carbonaceous residue in the product obtained after autoignition. The large exothermic peak due to the ignition reaction masks the peak corresponding to the crystallization of PLZT that usually appears as a small exothermic peak in the DTA curve. To estimate the enthalpy change (ΔH) of the ignition reaction, we performed DSC on the dried M−PVA gel of $R_{np} = 0.49$, and it was found to be (−)5.292 kJ/g. This enthalpy data is an indication of the exothermicity in the autoignition reaction of the M−PVA gel, which is many times lower than the exothermicity in the combustion reactions involving citrate−nitrate gel (−20 to −35 kJ/g)[20] that is often used to produce fine ceramic oxide particles.

B. Structural Characterization. Thermal analyses indicate a complete conversion of M−PVA gel to the product phase in a single-step autoignition reaction involving a low heat of reaction. However, to determine the phase composition and the particle size distribution of the product, we carried out XRD and TEM analyses.

Figure 2 shows the XRD patterns of the M−PVA gel-derived PLZT as-burnt powder from the autoignited gel with $R_{np} = 0.49$, annealed autoignited powder at 600 °C for 2 h in air, and dry gel with $R_{np} = 0.28$ calcined at 600 °C for 2 h in air in panels a−c, respectively. The XRD pattern in Figure 2a shows the presence of rhombohedral PLZT as the major phase, along with a peak of very small intensity corresponding to PbO(o). This suggests that the nano crystals of rhombohedral PZT are formed even in the as-burnt powder obtained after burning the gel on a hot plate at 180 °C. The as-burnt powder is yellow in color and contains negligible amounts of the carbonaceous part and hence an additional calcination step is not necessary in this modified PVA gel precursor route for the synthesis of the PLZT particle. Therefore, the as-burnt powder may be sintered directly for

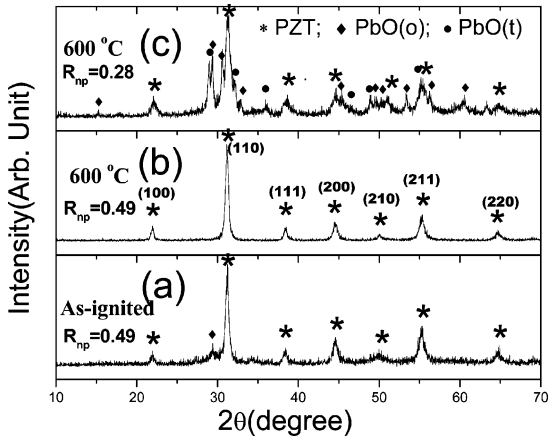

Figure 2. XRD patterns of the metal−PVA gel-derived PLZT, (a) as burnt powder from gel with $R_{np} = 0.49$ (b) annealed at 600 °C for 2 h in air, and (c) dry gel, with $R_{np} = 0.28$ calcined at 600 °C for 2 h in air.

consolidation without any further calcination. Earlier reports on the synthesis of nanocrystalline ceramic oxides from the M−PVA gel precursor showed that the gel burns incompletely on the hot plate and the as-burnt powder is black, full of carbonacious material, amorphous, and requires calcination at temperatures ≥600 °C to finally obtain the nanocrystalline material.[7,12−13] To study the effect of R_{np} on the autoignition efficiency of the gel and phase composition of the final product, we placed the gel with an R_{np} value of 0.28 in a glass beaker on the hot plate kept at 180 °C. It was observed that the gel with the aforementioned R_{np} could not be autoignited and hence required calcination at 600 °C for 2 h in air. The XRD pattern for this calcined sample shows the presence of rhombohedral PZT along with considerable amounts of unreacted PbO(t) and PbO(o) (Figure 2c). The single-phase rhombohedral PZT can be obtained only by annealing the powder at 600 °C for 6 h in air.

Figure 3a shows the TEM microstructure of the as-burnt powder obtained from gel with an R_{np} value of 0.49. The particles are extremely fine, with a narrow distribution of sizes between 1 and 6 nm. More than half of the particles have a size distribution within the range 1−1.5 nm. (Figure 4). Some of the particles are agglomerated and appear to be spherical with size ∼4−6 nm. The average particle size of the sample calculated from the TEM micrograph is 1.75 nm. Obtaining such a narrow size distribution of ultrafine particles by auto ignition of the M−PVA gel has marked advantages over the other chemical synthesis techniques. For example, the particle size of Pb-based perovskite oxides obtained by various methods are hydrothermal, 500 nm;[8] sol−gel, 30−60 nm;[10] citrate gel combustion, 50 nm;[6] polymer gel precursor, 20−25 nm;[12] homogeneous coprecipitation, 25 nm;[9] and peroxide-based route, 50 nm.[21] Compared to the well-known Pechini-type reaction,[22] the present methodology yields better results in that it yields finer particle size, narrower size distribution, and reduced agglomeration.

(20) Roy S.; Das Sharma, A.; Roy, S. N.; Maity, H. S. *J. Mater. Res.* **1993**, *8* (11), 2761−66.

(21) Camargo, E. R.; Popa, M.; Frantti, J.; Kakihana, M. *Chem. Mater.* **2001**, *13*, 1943−48.

(22) Gülgün M. A.; Popoola, O. O.; Kriven, W. M. *J. Am. Ceram. Soc.* **1994**, *77* (2), 531−39.

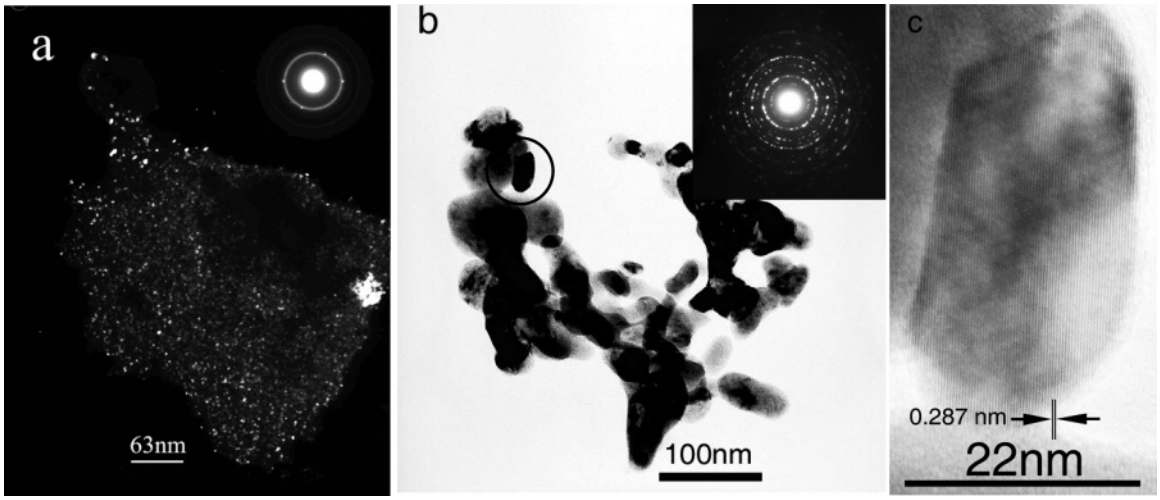

Figure 3. TEM micrograph of (a) as-burnt powder obtained by autoignition of gel with $R_{np} = 0.49$, dark-field and electron diffraction pattern inset; (b) gel with $R_{np} = 0.28$ calcined at 600 °C, bright-field and electron diffraction pattern (inset); and (c) HREM of the particle encircled in Figure 3b showing (110) planes of rhombohedral PLZT with an interplanar spacing of 0.287 nm.

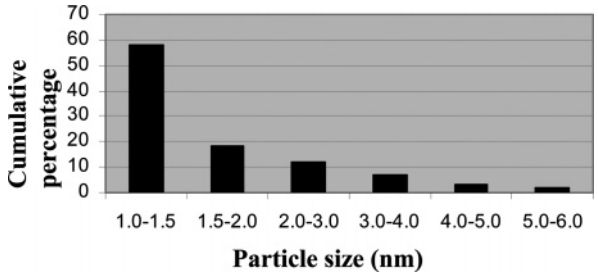

Figure 4. Particle size distribution of the PLZT sample in the TEM micrograph in FIgure 3a.

The d_{hkl} values calculated from the first four rings of the electron diffraction pattern shown in the inset of Figure 3b match with those of the (100), (110), (200), and (121) reflections of rhombohedral PLZT observed in the XRD pattern (Figure 2) at 0.405, 0.2905, 0.202, and 0.1675 nm, respectively. To get an idea of particle size distribution in the product obtained from gel with a lower R_{np} value, we performed TEM analyses on the PLZT powder obtained by calcining the dry gel with $R_{np} = 0.28$ at 600 °C for 6 h (Figure 3b). For this sample, calcination could not be avoided, as a gel of low R_{np} failed to experience autoignition. The particles in this powder sample exhibited faceted morphology and were much coarser compared to the ultrafine particles shown in Figure 3a. The average particle size of the finer particles in this sample is 25 nm, whereas the larger agglomerates have sizes in the range of 50−150 nm. From the electron diffraction pattern in the inset of Figure 3b, it appears that the sample is single phase with rhombohedral symmetry, which conforms to the XRD results.

To verify the reproducibility of this technique, we executed this synthesis technique a number of times for synthesis of PZT/PLZT and obtained reproducibility with respect to autoignition and speed of the reaction, with little variation in terms of agglomeration, particle size, and the amounts of unreacted PbO.

C. Synthesis Mechanism. The importance of using metal−polymer gel precursors in synthesizing nanomaterials of improved homogeneity lies in the random mixing of metal ions in solution at the atomic level. Metal ions added in the form of metal nitrates react with polymer in solution via the formation of a coordination complex through the O−H linkage present in the polymer, resulting in a homogeneous distribution of the metal ions. In dilute conditions, the reaction product is a very stable sol, which forms a gel when concentrated by thermal evaporation. The strong interaction between the OH groups and the metal ions helps maintain a homogeneous distribution of metal ions even after gel formation. Such an interaction, and the extremely high viscosity of the polymeric gel, prevents segregation of metal ions, resulting in a compositionally homogeneous gel. Cross-linking among the polymer chains, which increases the viscosity of the gel, is another important phenomena responsible for preventing metal segregation. However, it has been noticed that a high value of R_{np} imparts a negative effect on the cross-linking and hence regulating the value of R_{np} will be a compromise between the autoignitable exothermicity and homogeneity. It has also been noticed that if the pH of the M−PVA sol decreases below a certain level (i.e., a sol with a very high R_{np} value), the sol precipitates on thermal evaporation; hence, optimization of the pH of the M−PVA sol plays an important role in the stability of the sol.

According to the concept of propellant chemistry, a proper oxidizer/fuel molar ratio is needed for a stoichiometric ($\varphi = 1$) oxidizer/fuel mixture, which ensures complete combustion of the fuel.[23] The parameter φ is defined by the ratio of the oxidizing and reducing valencies of the oxidizer/fuel mixture. For the present M−PVA system, the total oxidizing valency of $Pb(NO_3)_2$, $TiO(NO_3)_2$, and $ZrO(NO_3)_2$ is 12 and the reducing valency of polyvinyl alcohol $[CH_2{=}CH(OH)]_n$ is 10, implying that a metal nitrate/PVA molar ratio of 1.2 is needed for $\varphi = 1$. This means that the nitrate/PVA molar ratio should be 2.4, as each mole of metal nitrate gives two moles of nitrate ions (NO_3^-). It is observed in the present experiment that the presence of such high nitrate concentration breaks the cross-linking of PVA in the M−PVA sol and thermal evaporation results in the formation of metal−

(23) Shea, L. E.; McKittrick, J.; Lopez, O. A. *J. Am. Ceram. Soc.* **1996**, *79* (12), 3257.

Table 1. Combustion Reaction Parameters Given in the Literature for Different Combustion Systems and a Comparison with the Present M−PVA System

reaction mode	smoldering combustion synthesis (SCS)	volume combustion synthesis (VCS)	SHS	M−PVA system
value of φ [24]	<0.7	0.7−1.2	01.2−1.6	0.13−0.6
T_{max}[a] (°C)	<600	1150−1350	800−1100	<∼700
self-propagation[24]	no	thermal explosion throughout	wavelike propagation	no
reaction duration[a, 25] (s)	100	10	20	up to 600
reaction initiation[24]	local	uniform throughout the mixture	local	local
as-burnt product[24−25]	amorphous	crystalline	crystalline	crystalline
carbonaceous part[24] (%)	Up to 20	1	1	0.65

[a] These parameters may vary to some extent for different fuels

PVA precipitate, which is detrimental for homogenization of the metal ions and for the stability of the M−PVA gel. Hence, in the present experiments, the oxidizer (NO_3^-)/fuel (PVA) molar ratio was kept at a much lower value of about 0.50. The equation for the M−PVA combustion reaction can be written as follows

$$12.9[CH_2{=}CH(OH)]_n(l) + 0.93Pb(NO_3)_2(l) + 0.07La(NO_3)_3(l) + 0.60ZrO(NO_3)_2(l) + 0.40TiO(NO_3)_2(l) + 2.0HNO_3(l) + 10.15O_2 + XH_2O(l) \rightarrow Pb_{0.93}La_{.07}Zr_{0.60}Ti_{0.40}O_3(s) + 25.8\,CO_2(g) + 3N_2(g) + XH_2O(g)$$

To understand the type of the combustion reaction that has taken place in the present system, we studied the ignition characteristics of the present reaction and the nature of the resulting as-burnt powder in light of the recently published results obtained from different combustion systems (Table 1).[24−26] Considering a very low value of φ and very long ignition duration, the present combustion synthesis ($\varphi < 0.7$) may be classified as smoldering combustion synthesis (SCS),[24] but the characteristics of the as-burnt powder in our case are different from that obtained by SCS. For instance, the SCS as-burnt product is amorphous, black, and carbonaceous and needs additional calcination for the crystallization as well as for the removal of the carbonaceous part. In contrast, the product obtained by the present synthesis method is well-crystalline PLZT and free from the carbonaceous part and does not need additional calcination for crystallization, which conform to the characteristics of the SHS product. The as-burnt powder in our case can be directly used for sintering. However, the ignition characteristics differ from that of SHS by the very low value of φ and the absence of self-propagation. The reaction in the present system starts at a certain point and engulfs the whole mixture very slowly, although the reaction cannot sustain if the heater is taken out. The present system may be called "modified SCS" (should not be confused with modified SHS) and has advantages over SCS of complete combustion of the fuel and crystalline product. The present system is an example of a fuel-rich oxidizer/fuel mixture (nonstoichiometric according to the hypothesis of propellant chemistry) that results in very slow but complete combustion.

The gel undergoes autoignition with the evolution of large amounts of gases such as H_2O, CO_2, N_2, and NO_3, leaving behind the porous fine voluminous residue with negligible amounts of the carbonaceous part (0.65 wt %, determined from the difference in weight between the as-ignited powder and the same calcined at 1000 °C). The degree of ignition reaction depends largely on the R_{np} value of the gel, because the polymer acts as fuel and the metal nitrates play the role of oxidizer. The gels with an R_{np} value between 0.46 and 0.53 underwent autoignition and got burned completely, producing yellow PLZT powder, whereas the gels with R_{np} values <0.46 underwent autoignition partially and failed to burn completely; this results in a black carbonaceous lumpy product, as the amount of oxidizer is insufficient for complete burning. Some of the gels with very low R_{np} values could not undergo autoignition at all. Although the hot plate was kept at 180 °C, the actual temperature within the pile of polymeric gel undergoing ignition depends on the stack arrangement and the gaseous atmosphere, i.e., oxygen content. The evolved gases during ignition also take part in dissipation of heat generated within the gel. Unlike the combustion reactions involving citric acid, glycine, hydrazine, etc., where there is a sudden pick up of temperature in the course of the reactions, the ignition of the M−PVA gel is sluggish and gets completed in about 10 min. The exposure of the product to this low ignition temperature for short duration minimizes particle growth and avoids high-temperature sintering of the product particles that are usually observed in the combustion synthesis using hydrazine,[17] urea,[16] glycine,[15] etc. A very high rate of nucleation of the complex oxide and a slow growth of the product nuclei are the possible reasons behind the formation of ultrafine particles.

D. Hazards and Feasibility of Large-Scale Production. Experimental observations and results of the thermal analyses indicate that the ignition of the M−PVA gel is slow and almost flameless, evolves nonpolluting gases such as CO_2 and N_2, and is much less vigorous than the combustion reactions involving glycine,[15] urea,[16] and hydrazine,[17] where the reactions are so vigorous that the ash particles are thrown violently through the combustion plume (Figure 3, Chick et al.[15]) and the reaction temperature reaches as high as 1450 °C.[15] Hence, proper safety arrangements are needed for large-scale production using the latter fuels. In contrast, the reaction at ∼300 °C can be performed inside a fume hood without any safety arrangement. Large-scale production of lead-based perovskite oxides using M−PVA gel would not involve any risk factor, as the reaction is supposed to be carried out in

(24) Mukasyan, S.; Costello, C.; Sherlock, K. P.; Lafarga, D.; Varma, A. *Sep. Purif. Technol.* **2001**, *25*, 117
(25) Deshpande, K.; Mukasyan, A.; Varma, A. *J. Am. Ceram. Soc.* **2003**, *86* (7), 1149−54.
(26) Deshpande, K.; Mukasyan, A.; Varma, A. *Chem. Mater.* **2004**, *16*, 4896.

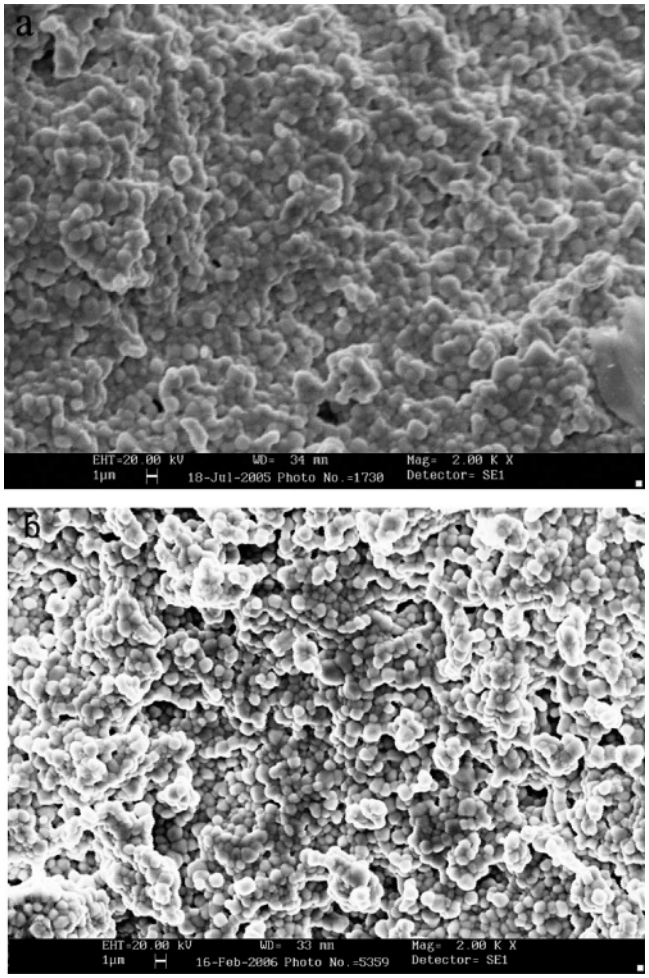

Figure 5. SEM micrograph taken on the fractured surface of PLZT pellets sintered at (a) 1100 and (b) 1200 °C for 4 h.

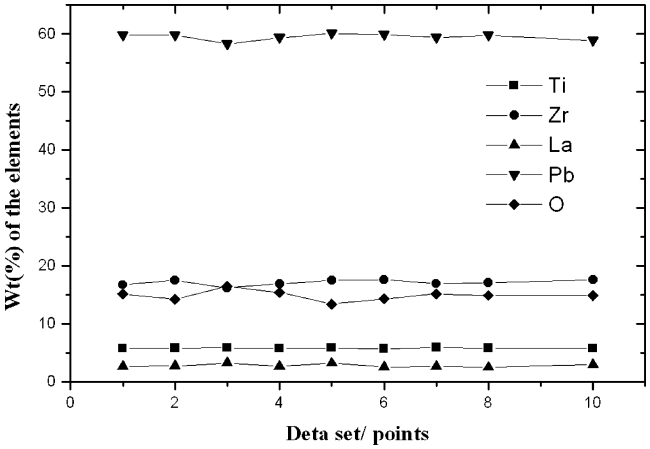

Figure 6. Quantitative estimation of the elements in the sintered PLZT pellet by EPMA.

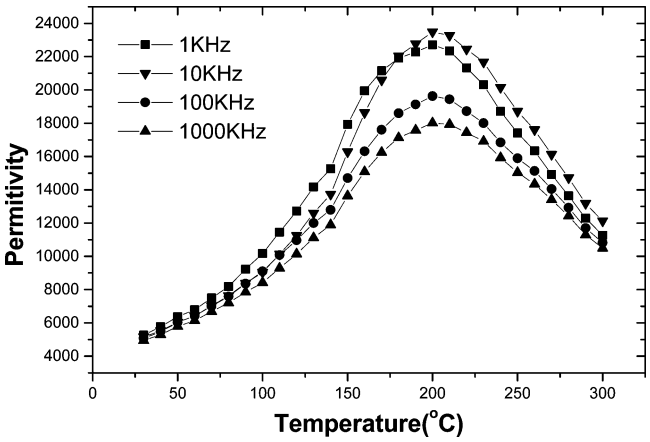

Figure 7. Dielectric permittivity (κ) vs temperature curves at different frequencies for the 1100 °C sintered PLZT sample.

an open vessel. Evolution of a large quantity of gas does not pose a threat, as the gases eject easily through the porous structure of the dried gel undergoing ignition. The ignition process progresses slowly and there is no sudden generation of large quantity of gas at any point of time. Synthesis of powdered ceramic oxides with minimized agglomeration may also be carried out by spray pyrolysis of concentrated M−PVA sol. Moreover, the process exploits the advantages of using an inexpensive chelating agent (PVA), $ZrCl_4$, and $TiCl_4$, instead of expensive Ti-alkoxides. The reproducibility of this single-step synthesis procedure has been proved by a number of successful attempts in producing ultrafine PZT and PLZT powders.

E. Sintering and Densification. The pellets made from as-burnt powdered sample obtained from M−PVA gel with $R_{np} = 0.49$ and average particle size 1.75 nm were sintered at 1100 and 1200 °C for 4 h in air. The samples could be sintered to 94 and 96% of their theoretical density at those temperatures.

The SEM micrograph taken on fractured portions of the 1100 °C sintered sample is shown in Figure 5a. The micrograph shows the distribution of grain sizes in the size range 0.4−1.2 μm. The grain size does not increase significantly on increasing the sintering temperature to 1200 °C (Figure 5b).

Although the chemicals are added in the stoichiometric ratio, the synthesis of $ZrO(NO_3)_2$ and $TiO(NO_3)_2$ from $ZrCl_4$ and $TiCl_4$ involves some steps in which the stoichiometry could be lost before reaching the final step. Hence, electron probe microanalysis (EPMA) was performed on the polished sintered pellets for quantitative estimation of the elements in the sintered samples. Microanalysis data were acquired on nine arbitrary points on the polished and carbon-coated sample. The results obtained from the 1100 °C sintered $Pb_{0.93}La_{0.07}Zr_{0.60}Ti_{0.40}O_3$ (PLZT 7/60/40) sample originally comprising Pb, 59.43; La, 2.99; Zr, 16.88; and Ti, 5.88 wt %, are plotted and shown in Figure 6. The results show a very good homogeneity, as expected, with respect to the elements Pb, La, Zr, Ti, and O present throughout the sample, although the figure shows little variation in the line plots. The very small variation in stoichiometry at different points is as expected and usually occurs in the sample that is not polished perfectly to yield a microscopic flat surface. These variations are well within the error limit of EPMA quantitative measurements.

F. Dielectric Properties. *1. Relative Permittivity.* Figure 7 shows dielectric permittivity (κ) vs temperature (T) curves at four different frequencies for the 1100 °C sintered sample, the SEM microstructure of which is shown in Figure 5. The value of dielectric permittivity for the sample at room temperature is much higher (∼5000) than either the values

reported for the similar sample synthesized by a conventional solid-state method with the same composition[27] ($\kappa = 2590$) or fine-grained PLZT5/54/46 derived from mechanical alloying ($\kappa = 1200$ at grain size $>1\mu$m and 2000 at grain size ~ 0.5 μm).[28] Earlier studies revealed that the change in dielectric permittivity with grain size is different in different ranges of grain size. For grains having sizes <1 μm, dielectric permittivity increases with increasing grain size, showing a maximum at ~ 1 μm, and then decreases with increasing size for grains >1 μm[19]. Buessem et al.[29] explained anomalously high permittivity in fine-grained $BaTiO_3$ ceramic by the absence of 90° twining within the grains of size ≤ 1 μm, giving rise to internal stresses as the ceramic cools below the curie temperature, whereas Arlt et al.[19] studied the variation of domain size with grain sizes experimentally and showed that 90° domains exist in the fine-grained $BaTiO_3$ grains of sizes down to 0.7 μm. The high dielectric permittivity of the samples consisting of grains of ~ 1 μm is attributed to the increased contribution of 90° domain walls to the dielectric permittivity. The permittivity of fine-grained ceramics is believed to be the sum of volume contruibution, i.e., permittivity of single-crystal dielectric and contribution of the 90° domain walls.[19] The room-temperature dielectric permittivity of the 1200 °C sintered sample is much lower ($\sim$800) than that of the 1100 °C sintered sample. The abrupt decrease in permittivity cannot be correlated to the increase in grain size, as there is no obvious increase in grain size on increasing the sintering temperature from 1100 to 1200 °C. This can, however, be interpreted by the micro-inhomogeneity developed because of higher lead (Pb) loss at 1200 °C. The Pb deficiency in the sample sintered at 1200 °C was confirmed by XRD measurements. To verify the validity of this assumption, we milled one PLZT sample with 5 mol % extra PbO and sintered it at 1200 °C for 4 h. It was assumed that extra PbO would compensate the lead loss in sintering at 1200 °C. The measured room-temperature dielectric permittivity for this sample is $\sim$3000. Hence, from these results, it appears that the low dielectric constant ($\sim$800) of the 1200 °C sintered sample is attributed to micro-inhomogeneities developed because of Pb loss from the PLZT sample sintered at higher temperature.

The Curie point (200 °C) observed for the 1100 °C sintered sample is higher than that reported earlier for the coarser grain PLZT with the same composition (160 °C).[27] However, this difference in Curie temperature cannot be explained as an effect of particle size, as the Curie point shows only a little variation due to the change in particle size in micrometer-sized grains.[30]

2. Diffused Phase Transition. From Figure 7, it is observed that the sample undergoes a diffuse phase transition (DPT) from the ferroelectric to paraelectric phase with a broadened $\kappa-T$ peak at 200 °C. Ferroelectrics with diffuse phase transitions are usually characterized by the appearance of a broad ferroelectric to paraelectric phase-transition region. Moreover, they show a dispersion of maximum relative dielectric permittivity as a function of frequency. Ferroelectric to paraelectric phase transitions with a broadened peak in the $\kappa-T$ plot for ferroelectric materials with small grain size were reported earlier.[28−32] For practical applications, an increasing trend of exploiting the advantages of maximum relative dielectric permittivity over a range of temperatures has been noticed. For the present PLZT sample, apart from peak broadening, both κ vs T and tan δ vs T plots (Figure 8) show marked frequency dispersion. However, the peak temperature in the $\kappa-T$ plot does not show any change with frequency, indicating a nonrelaxor behavior. Okazaki et al. reported a similar kind of diffused phase transition observed for the hot-pressed PLZT 8/65/35 with particle sizes ranging from 1 to 2 μm.[31] The dielectric permittivity of a classical ferroelectric above the Curie point follows the Curie−Weiss law.[1,2]

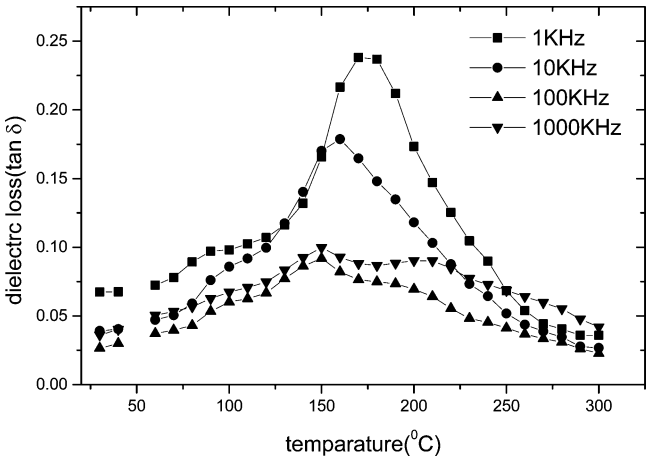

Figure 8. Dielectric loss (tan δ) vs temperature curves at different frequencies for the 1100 °C sintered PLZT sample.

$$\kappa = C/(T - T_c) \tag{1}$$

where, κ is the dielectric permittivity, C is the Curie−Weiss constant, and T_c is the curie temperature. For ferroelectrics with diffused phase transition, the deviation from Curie−Weiss law is measured by fitting the $\kappa-T$ curve at the temperature range of $T > T_{max}$ with the following modified Curie−Weiss equation[33]

$$1/\kappa - 1/\kappa_{max} = C^{-1}(T - T_{max})^{\gamma} \tag{2}$$

where κ_{max} is the maximum dielectric constant at T_{max} and γ is the critical exponent; $\gamma = 1$ for a classical Curie−Weiss ferroelectric and $\gamma = 2$ for systems with a completely diffused phase transition.

The value of γ has been determined from the slope of the straight line fitted to the logarithmic plot ln $(1/\kappa - 1/\kappa_{max})$ vs ln$(T - T_{max})$. For the present 1100 °C sintered PLZT sample, the values of γ are found to be 1.75, 1.97, 1.85, and 2.07, respectively, at 1, 10, 100, and 1000 kHz frequencies, indicating completely diffused phase transitions.

(27) Haertling, G. H. *J. Am. Ceram. Soc.* **1999**, *82* (4), 797−818.
(28) Takagi, K.; Kikuchi, S.; Li, J.-F.; Okamura, H.; Watanabe, R.; Kawasaki, A. *J. Am. Ceram. Soc.* **2004**, *87* (8), 1477−1482.
(29) Buessem, W. R.; Cross, L. E.; Goswami, A. K. *J. Am. Ceram. Soc.* **1966**, *49* (1), 33−36.
(30) Randall, C. A.; Kim, N.; Cao, J.-P. K. W.; Shrout, T. R. *J. Am. Ceram. Soc.* **1998**, *81* (3), 677−88.
(31) Okazaki, K.; Nagata, K. *J. Am. Ceram. Soc.* **1971**, *56* (2), 82−86.
(32) Kinoshita, K.; Yamaji, A. *J. Appl. Phys.* **1976**, *47* (1), 371−373.
(33) Uchino, K.; Nomura, S. *Ferroelectr. Lett.* **1982**, *44*, 55−61.

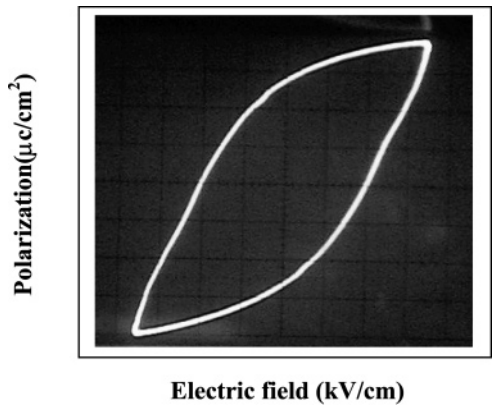

Figure 9. Room-temperature $P-E$ hysteresis loops of the PLZT sample at 50 Hz.

Figure 8 shows dielectric loss (tan δ) vs temperature curves at four different frequencies for the 1100 °C sintered sample. The dielectric losses of the sample at room temperature at 100 and 1000 kHz are found to be <2.5%, and for the entire frequency range it remains <4.6%. The obtained values of dielectric losses are comparable to that reported in literature for the PLZT samples with similar compositions but synthesized by a conventional solid−state method. The dielectric losses reported for PLZT 7/60/40 ($\kappa = 2590$), PLZT 8/65/35 ($\kappa = 3400$), and PLZT 9/65/35 ($\kappa = 5700$) are 1.9, 3.0, and 6%, respectively.[27] At 100 and 1000 kHz frequencies, the tan $\delta-T$ peaks are depressed and almost flat, which shows the dielectric quality of the sample at these frequencies.

Figure 9 shows the hysteresis loop at room temperature of the PLZT sample sintered at 1100 °C. A high electric field of 30 kV/cm was required in order to obtain saturation polarization. The values of remnant polarization (P_r) and coercive field (E_c) of the material were determined from its hysteresis loop. It has been observed that the room-temperature hysteresis loop has a well-defined squareness and is of memory type.[1] The numerical value of remnant polarization and coercive field at saturation are 34.6 μc/cm^2 and 7 kV/cm, respectively. The value of remnant polarization obtained is comparable to the values usually obtained from PLZT samples processed by conventional solid-state method (~30 μc/cm^2).[27]

IV. Conclusions

Autoignitable M−PVA gel could be obtained by maintaining the proper PVA/ NO_3^- ratio in the gel, which burns completely on a hot plate to offer ultrafine ceramic powder with an average particle size of 1.75 nm, leaving negligible carbonaceous residue. The ignition of M−PVA gel exhibited low exothermicity, which helped in avoiding particle coarsening. The as-burnt powder obtained after ignition could be sintered directly for consolidation to 94 and 96% of the theoretical density. Elemental analysis by EPMA showed excellent homogeneity of the sintered PLZT samples. The 1100 °C sintered sample showed a very high dielectric permittivity of ~5000, which decreases drastically to ~800 for the 1200 °C sintered sample. The generation of microinhomogeneity due to lead loss resulting from high-temperature sintering proved detrimental for dielectric properties of the sintered PLZT samples. The sintered PLZT sample underwent completely diffused phase transition from ferroelectric to paraelectric phase at around 200 °C. The remnant polarization and coercive field at saturation for the 1100 °C sintered PLZT sample were found to be 34.6 μc/cm^2 and 7 kV/cm. The process exploits the advantages of simple chemical methodology, inexpensive precursors, and a high degree of reproducibility and shows good potential for large-scale production of single- or multicomponent ultrafine ceramic oxides.

Acknowledgment. The authors thankfully acknowledge the financial support from the Defense Research Development Organization, Ministry of Defense, New Delhi, for carrying out the present work and thank the Director of DMRL for his constant encouragement. The help of Dr. A. K. Singh and Mr. V. V. Rama Rao, Scientists at DMRL, Hyderabad, in obtaining EPMA measurements and Dr. Abhijit Roy, Universität Duisburg−Essen Standort Duisburg, for helpful discussions is gratefully acknowledged.

CM061884+